• Letter to the Editor •

Angle closure glaucoma in a patient with X-linked retinoschisis: a case report

Lu Yao[1,2,3], Ye Lu[1,2], Kang-Yi Yang[1,2], Kun Lyu[1,2], Zong-Yi Wang[1,2], Lyu-Zhen Huang[1,2], Hui-Juan Wu[1,2]

[1]Department of Ophthalmology, Peking University People's Hospital, College of Optometry, Beijing 100044, China

[2]University Health Science Center; Beijing Key Laboratory of Diagnosis and Therapy of Retinal and Choroid Diseases, Beijing 100044, China

[3]Department of Ophthalmology, Air Force Medical Center, Affiliated Hospital of Air Force Medical University, Beijing 100142, China

Co-first authors: Lu Yao and Ye Lu

Correspondence to: Hui-Juan Wu. Peking University People's Hospital, College of Optometry, Beijing 100044, China. dr_wuhuijuan@126.com

Dear Editor,

X-linked retinoschisis (XLRS) is a rare X-linked recessive disorder predominantly afflicting young males. The schisis of the retinal layers is a result of deleterious mutations in the *RS1* gene. Insufficient epidemiological data has caused significant variation in reported global prevalence, with estimates fluctuating between 1 in 5000 and 1 in 30 000 individuals[1]. A large follow-up multicenter study recently published has yielded noteworthy findings concerning the phenotypic spectrum, long-term natural history, and genotype of XLRS. The investigation revealed a significant variability in visual function and disease progression, with particular variants of the *RS1* gene displaying diverse phenotypic expressions, suggesting the intricate genetic basis underlying this disorder[2]. The range of visual impairments associated with XLRS is extensive, varying from minor to severe. This condition is also characterized by specific retinal abnormalities, including radial streaks emanating from a divided central fovea, schisis affecting the inner layers of the retina in peripheral areas, and a diminished amplitude ratio of b- to a-wave, or even an electronegative electroretinography (ERG)[3]. At their initial consultation, the majority of individuals with XLRS exhibit visual acuity (VA) levels between 20/60 and 20/120. However, there is a significant diversity in the condition's presentation and progression, even among relatives, with VA levels spanning from near-normal to complete loss of sight[4-5]. While vision tends to be reasonably consistent over several years for those with XLRS, there is documentation of a more rapid decline in later adulthood, specifically during the fourth and fifth decades, due to central retinal degeneration[5-7]. Moreover, those with XLRS face an elevated risk for serious visual issues, such as retinal detachment, vitreous hemorrhages, and neovascular glaucoma[4]. Female carriers could be found with slightly abnormal retinal changes without clinical symptoms[5]. Even within the same family, the manifestation and progression of the condition can vary greatly, with individuals experiencing anything from nearly normal vision to complete loss of sight[8-9]. Earlier investigations have revealed that retinoschisis-related cystoid degeneration can impact multiple layers of the retina, beginning at the retinal nerve fiber zone and continuing to the nuclear stratum, with considerable fluctuation in the severity of the schisis[10-13].

Refractory angle-closure glaucoma (ACG) has been described previously in patients with XLRS[9-10]. Furthermore, cases of XLRS in adolescents with ACG have been reported before[11-12]. However, cases of XLRS in young adult men with non-refractory glaucoma have been rarely reported as far as we know.

Here we report a 28-year-old male with ACG and genetically confirmed XLRS. This case report provides a unique perspective on the relationship between XLRS and ACG and could help guide future research and clinical management of patients with these conditions. The study received clearance from the Ethics Committee of Peking University People's Hospital, China, under the reference number 2022PHB256-001, and the patient granted written consent for the publication of the case narrative and associated imagery.

CASE PRESENTATION

A 28-year-old male reported a history of bilateral blurred vision due to anisometropia spanning ten years. Additionally,

he has been experiencing periodic ocular discomfort and visual phenomena resembling flickering lights in both eyes (BE) for the last two months. Over an extended timeframe, a comprehensive series of eye examinations were conducted on him, including detailed retina inspections, anterior segment ultrasound biomicroscopy (UBM), optical coherence tomography (OCT) of macular, fluorescein fundus angiography (FFA), and field of vision evaluation utilizing Humphrey perimetry.

The patient first visited the local hospital 9 years ago. At the outset of the ophthalmic evaluation, the optimal-corrected VA (OCVA) was determined to be 20/125 bilaterally, indicating a level of vision that falls within the moderate to severe impairment category. The intraocular pressure (IOP) measurements revealed 21 mm Hg in the right eye and 25 mm Hg in the left eye, indicating a marginal elevation in the latter. The slit-lamp biomicroscopy disclosed no noteworthy irregularities in the ocular surface structures and anterior segment of BE, involving the conjunctival, corneal, and lenticular structures. The depth of the central anterior chamber was found to be within the normal range, whereas the peripheral anterior chamber exhibited shallowness in BE. The fundus photograph of BE demonstrated microcystic-like changes of the macular region, with cup size to disc size ratios of 0.2 in the right eye and 0.4 in the left eye, rendered in Figure 1A and 1B. The OCT scan of the macula revealed that retinoschisis predominantly affected the retinal nerve fiber zone and the inner nuclear stratum, as illustrated in Figure 1C and 1D. The perimetry test revealed no typical visual field loss of BE. The diagnoses of congenital macular degeneration and glaucoma suspect were given at that time. The patient was then managed with anti-glaucoma eye drops (timolol and travoprost) to control ocular tension. But he did not take regular eye check-ups since then.

In this visit, the OCVA was 20/125 and 20/80, and IOP measurements were 21 and 34 mm Hg in right and left eyes, respectively. The anterior ocular segment of BE appeared unexceptional barring the presence of a narrow peripheral anterior chamber. The cup to disc ratios exhibited a moderate uptick compared to the measurements taken 9y prior. Gonioscopy classified and recorded with the Scheie grading system demonstrated that the anterior chamber angle of BE was grades III at the inferior quadrant and grades IV at other quadrants in static condition (Figure 2C, 2D), and the dynamic assessment revealed that the anterior chamber angles were partially patent in the inferior and nasal anterior chamber of the right eye and the inferior anterior chamber of the left eye. No new blood vessels were observed on the iris or within the angle, no adhesions between the iris and lens occurred, and the iris did not exhibit a bombe configuration. Anterior
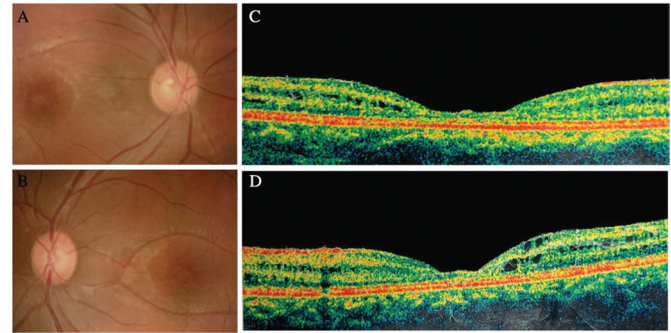
Figure 1 Fundus photograph and macular lutea scans of the patient 9 years ago using optical coherence tomography A, B: Fundus images of right and left eyes separately; C, D: Macular lutea scans of right and left eyes using optical coherence tomography.
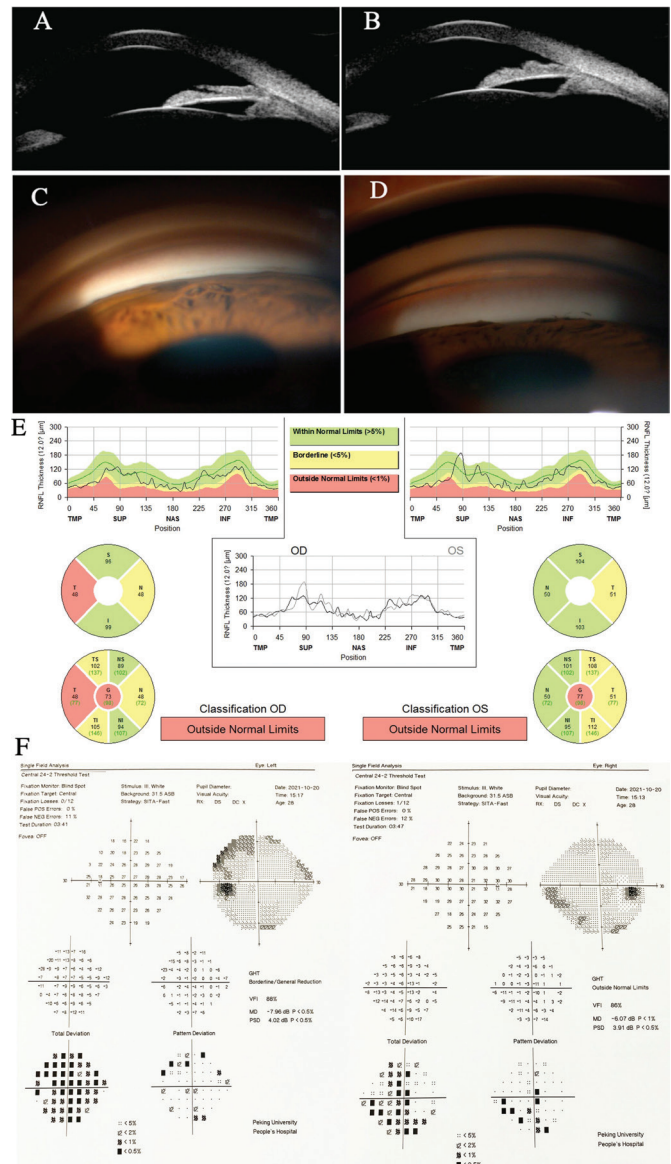

Figure 2 Ultrasound biomicroscope, gonioscopy, retinal nerve fiber zone around optic papilla and perimeter results A, B: Ultrasound biomicroscope images of right and left eyes indicated a closed angle in the anterior chamber; C, D: Gonioscopy prism examination of right and left eyes at the inferior quadrant; E: Retinal nerve fibre zone around the optic nerve papilla measured by spectral domain optical coherence tomography; F: Perimeter testing results of left and right eyes.

segment UBM (Aviso, Quantel Medical, Inc., Bozeman, MT, USA) test showed the anterior chamber angles of BE were closed in all directions (Figure 2A, 2B). Biometric data was acquired by IOL Master to eliminate cataractous angle-closure, which revealed the ocular axial lengths (AL) to be 21.68 and 21.76 mm, lenticular thickness of 4.15 and 4.23 mm, anterior chamber depths of 2.83 and 2.64 mm in right and left eyes, respectively. The retinal nerve fibre layer around the optic nerve head was thinner than normal of BE measured by spectral domain OCT (SD-OCT, Heidelberg Engineering, Heidelberg, Germany; Figure 2E), and defects in the visual field were identified in BE using the SITA 24-2 program on the Humphrey Field Analyzer 750i from Carl Zeiss Meditec in Dublin, CA, USA. Fundus photographs of BE were notable for microcystic-like changes in the macular area (Figure 3A, 3B) which had no obvious change compared with the fundus photographs 9 years ago. OCT images of BE presented atrophy of the fovea while the retinoschisis in macular area was not obvious (Figure 3C, 3D) with the central macular thickness (CMT) of 370 and 477 μm in right eye and left eye, respectively. However, retinoschisis in the inner layers of the retina was discerned in the peripheral area (Figure 3E, 3F). Autofluorescence of BE was detected in the macular area with a patch pattern of high fluorescences (Figure 3G, 3H). FFA of BE indicated hyper-illuminated window defects in the macula lutea (Figure 3I, 3J). The ERG revealed a decrease in b-wave amplitude for BE in the scotopic ERG, diminished a-wave and b-wave in the photopic ERG, and reduced amplitude in the 30 Hz flicker response. High-throughput sequencing examination revealed that the patient carried the NM_000330 (RS1), exon6: c.626G>A (p.R209H) mutation. Sanger sequencing was conducted to validate the genetic status of the proband and his kinfolks, as depicted in Figure 4B. The presence of one copy of the *RS1* gene variant was verified in his mother (chrX:18660173), whereas no such variant was identified in either his father or female sibling. The family lineage was illustrated in Figure 4A. His mother showed no significant ocular findings. No noteworthy ocular abnormalities were observed in his mother.

A diagnosis of XLRS and ACG of BE was made. Carteolol hydrochloride and brimonidine tartrate ophthalmic solutions were administered to relieves the patient's ocular hypertension. Then the IOP of the patient were decreased to 19 and 18 mm Hg in right and left eyes, respectively, the OCVA was 20/125 of right eye and 20/80 of left eye, and regular follow-up checks were conducted.

MOLECULAR GENETIC METHODS

Blood samples of 3 to 5 mL, collected from the peripheral veins of the subjects, were treated with ethylenediamine tetraacetic acid (EDTA) to prevent clotting. DNA, with a
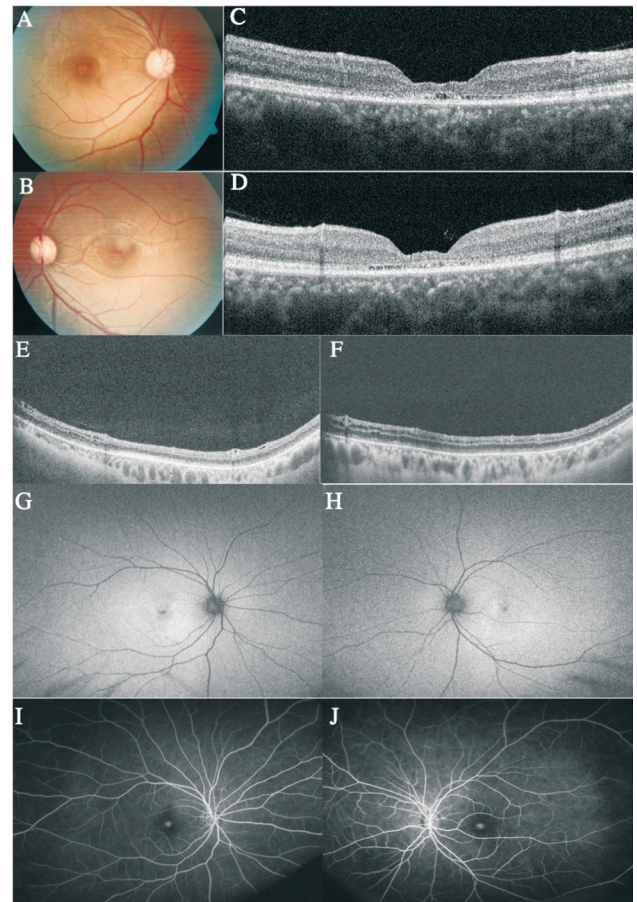
Figure 3 Series of fundus examinations of right and left eyes A, B: Fundus photographs; C, D: Macular lutea scans using spectral domain optic coherence tomography; E, F: The peripheral retina scans using spectral domain optic coherence tomography; G, H: Ocular autofluorescence captures; I, J: Fluorescein angiography visualizations.
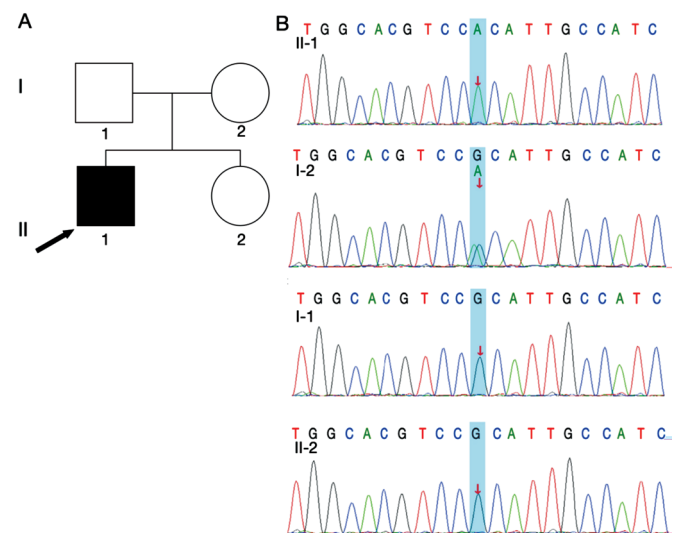
Figure 4 Sanger sequencing analysis was employed to pinpoint the family's lineage and the mutation A: In the family tree, those with X-linked retinoschisis are marked by solid symbols, while clinically unaffected individuals are represented by hollow circles or squares. The figures below the symbols denote the sibship numbers for each person. The arrow points to the index case within the family (II-1). B: Characteristic sequence traces are presented for II-1 (hemizygous for the mutation), I-2 (heterozygous mutation carrier), I-1 (unmutated type), and II-2 (unmutated type). The *RS1* gene reference is NM_000330.

concentration of at least 20 ng/μL, was extracted using the silica gel membrane technology and a rapid centrifugation column method, employing the QIAamp DNA Blood Midi Kit from Qiagen (Hilden, Germany). The purity of the genome DNA was assessed through ultraviolet spectrophotometry and confirmed by agarose gel-based electrophoresis. For exome sequencing, 1-3 μg of genomic DNA was sheared into fragments averaging 180 bp in length using a Bioruptor sonicator (Diagenode) by MyGenostics Incorporation in Beijing, China, which was sourced from the sample[14]. Following linear expansion *via* polymerase chain reaction (PCR), the collection of cDNA sequences underwent verification and sequencing. After sequencing, raw data were finely filtered to obtain clean reads. The sequencing depth and coverage of the target region were assessed by aligning filtered reads to the reference genetic blueprint. Subsequently, the filtered reads were aligned to the human genomic sequence utilizing the Burrows-Wheeler Aligner (BWA) software. Single nucleotide variants (SNVs) and insertions and deletions (InDels) were detected by software called GATK and VarScan. After above two steps, the data would be transformed to VCF format, variants werefootnoted by ANNOVAR subsequently and tied to various databases, such as 1000 genome, ESP6500, dbSNP, EXAC, Inhouse (MyGenostics), HGMD, and forecast by SIFT, PolyPhen-2, MutationTaster, GERP++[15]. Before follow-up analysis, necessary emission sample filtering and pedigree analysis filtering were carried out on the variant data set.

Genetic specimens from other three examinees of this lineage were screened for the existence of the mutation using Sanger sequencing. For PCR-induced amplification, primers sequences were developed targeting the previously identified mutant sites. The PCR replication reaction system was configured by using the preconfigured program of the Beckman automated workstation, and replication was carried out by using an A&B PCR instrument under the following conditions: an initial denaturation at 98℃ for 2min; followed by 10 cycles of 98℃ for 10s, 65℃ for 30s, and 72℃ for 10s; then 25 cycles of 98℃ for 10s, 55℃ for 30s, and 72℃ for 10s; finally, the samples were refrigerated at 4℃. The products were sequenced by Sanger sequencing. In select kin, the cosegregation of mutated gene loci was authenticated to ascertain which specific gene loci were responsible for *RS1* within the siblings and parents.

DISCUSSION

In this case, the young man had a rare combination of XLRS and ACG with NM_000330 (RS1), exon6: c.626G>A (p.R209H) mutation and the genetic variation segregated in the mother (chrX:18660173) and the affected individual, but no *RS1* gene variation was detected in his sister and father. At the molecular dimension, the pathological condition is intertwined with alterations in the *RS1* gene situated at Xp22, encoding

retinoschisin, a secretory protein containing a discoidin-like domain[5]. Retinoschisin is currently believed to be a functional protein to target cellular fluid homeostasis, cellular adhesion, and synaptic interactions between bipolar and photoreceptor cells[16]. Cystoid alterations in multiple retinal layers can stem from the deficiency of retinoschisin[5]. Recent study also revealed that entrapment of mutant retinoschisin protein within photoreceptor inner segments as well as disrupted reciprocal regulation between L-type voltage-gated calcium channels and retinoschisin contribute to the dysfunction in photoreceptors[17].

This case is unique because our patient did not have any secondary factors of ACG compared to the patients in other reported cases[18-20]. Anatomical categorization of angle-closure contains iris-pupil obstruction, plateau iris syndrome/non-pupillary block, lens-induced angle-closure, and retrolenticular factors, *etc*. Most previously reported cases had specific secondary retrolenticular factors of ACG, peripheral retinal detachment. Huang *et al*[18] characterized recurrent glaucoma in a case of retinoschisis with R102W RS1 mutation and peripheral retinal schisis. Low *et al*[19] reported a case of XLRS with refractory ACG in a 39-year-old man, which is secondary to the mixed mechanisms (pupil block, plateau iris/non-pupil block, lens-induced angle-closure, and exudative retinal detachment). Selvan *et al*[20] described a rare phenotype of XLRS with ACG in an 11-year-old boy who also had peripheral retinoschisis. There existed peripheral fundus lesions in all the cases mentioned above and their conditions were relatively intricate. However, in our case, the patient had no abnormality in the peripheral retina. Moreover, the course of ACG in our patient was more stable compared with other cases. Of note, most proband patients[18-19,21] were characterized by short eye AL and narrow anterior chamber. These findings indicated that the early onset of ACG in XLRS patients may be due to anatomical morphology such as short eye AL and narrow anterior chamber elicited by the *RS1* gene mutation. However, our patient only had short eye AL and his anterior chamber is not shallow. Thus, the biological processes that explain the connection between retinal irregularities and ACG warrant additional investigation.

Unlike other previously reported cases[19-21], our proband used α receptor agonists for the first time, which manifested a passable effect on our patient. Obvious adverse effects were also undetected. Nevertheless, there is a lack of substantial data regarding the long-term safety and effectiveness of alpha-agonistic agents in patients with XLRS and ACG.

In conclusion, although XLRS associated with ACG was not common, gonioscopy and relevant examinations should be conducted in patients with short AL and shallow anterior chamber depth.

REFERENCES

1 Grigg JR, Hooper CY, Fraser CL, *et al*. Outcome measures in juvenile X-linked retinoschisis: a systematic review. *Eye* (*Lond*) 2020;34(10):1760-1769.

2 Hahn LC, van Schooneveld MJ, Wesseling NL, *et al*. X-linked retinoschisis: novel clinical observations and genetic spectrum in 340 patients. *Ophthalmology* 2022;129(2):191-202.

3 Pennesi ME, Birch DG, Jayasundera KT, *et al*. Prospective evaluation of patients with X-linked retinoschisis during 18 months. *Invest Ophthalmol Vis Sci* 2018;59(15):5941-5956.

4 Pimenides D, George ND, Yates JR, *et al*. X-linked retinoschisis: clinical phenotype and RS1 genotype in 86 UK patients. *J Med Genet* 2005;42(6):e35.

5 Molday RS, Kellner U, Weber BH. X-linked juvenile retinoschisis: clinical diagnosis, genetic analysis, and molecular mechanisms. *Prog Retin Eye Res* 2012;31(3):195-212.

6 Apushkin MA, Fishman GA, Rajagopalan AS. Fundus findings and longitudinal study of visual acuity loss in patients with X-linked retinoschisis. *Retina* 2005;25(5):612-618.

7 Orès R, Mohand-Said S, Dhaenens CM, *et al*. Phenotypic characteristics of a French cohort of patients with X-linked retinoschisis. *Ophthalmology* 2018;125(10):1587-1596.

8 Huang L, Sun LM, Wang ZR, *et al*. Clinical manifestation and genetic analysis in Chinese early onset X-linked retinoschisis. *Mol Genet Genomic Med* 2020;8(10):e1421.

9 Smith LM, Cernichiaro-Espinosa LA, McKeown CA, *et al*. X-linked peripheral retinoschisis without macular involvement: a case series with *RS1* genetic confirmation. *Ophthalmic Genet* 2020;41(1):57-62.

10 Gerth C, Zawadzki RJ, Werner JS, *et al*. Retinal morphological changes of patients with X-linked retinoschisis evaluated by Fourier-domain optical coherence tomography. *Arch Ophthalmol* 2008;126(6):807-811.

11 Gregori NZ, Berrocal AM, Gregori G, *et al*. Macular spectral-domain optical coherence tomography in patients with X linked retinoschisis. *Br J Ophthalmol* 2009;93(3):373-378.

12 Yu J, Ni YQ, Keane PA, *et al*. Foveomacular schisis in juvenile X-linked retinoschisis: an optical coherence tomography study. *Am J Ophthalmol* 2010;149(6):973-978.e2.

13 Wei X, Li H, Zhu T, *et al*. Genotype-phenotype associations in an X-linked retinoschisis patient cohort: the molecular dynamic insight and a promising SD-OCT indicator. *Invest Ophthalmol Vis Sci* 2024;65(2):17.

14 Kong LH, Chu GM, Ma W, *et al*. Mutations in *VWA8* cause autosomal-dominant retinitis pigmentosa *via* aberrant mitophagy activation. *J Med Genet* 2023;60(10):939-950.

15 Luo HD, Pei SN, Wang AJ, *et al*. A pedigree with retinitis pigmentosa and its concomitant ophthalmic diseases. *Int J Ophthalmol* 2023;16(12):1962-1970.

16 Smit-McBride Z, Sun N, Thomas S, *et al*. Kir4.1 and Aqp4 contribution to schisis cystic water accumulation and clearance in the Rs1 exon-1 del XLRS rat model. *Genes* 2024;15(12):1583.

17 Ambrosio L, Akula JD, Harman JC, *et al*. Do the retinal abnormalities in X-linked juvenile retinoschisis include impaired phototransduction? *Exp Eye Res* 2023;234:109591.

18 Huang XF, Tu CS, Xing DJ, *et al*. R102W mutation in the RS1 gene responsible for retinoschisis and recurrent glaucoma. *Int J Ophthalmol* 2014;7(1):169-172.

19 Low S, Mohamed R, Ting M, *et al*. The treatment of refractory angle-closure glaucoma in a patient with X-linked juvenile retinoschisis. *Ophthalmic Genet* 2018;39(5):625-627.

20 Selvan H, Sharma A, Birla S, *et al*. Molecular characterization of a rare phenotype of X-linked retinoschisis with angle-closure glaucoma. *Indian J Ophthalmol* 2019;67(7):1226-1229.

21 Li YX, Li J, Pan XZ, *et al*. Management of angle-closure glaucoma with X-linked retinoschisis: a case report. *BMC Ophthalmol* 2023;23(1):159.